Carbon Nanotube Based Aqueous Ion and pH Sensor

Suchit Bhattarai, Konrad H. Aschenbach, Dr. Romel D. Gomez

Abstract— **This study characterizes the response of carbon nanotube (CNT) based biosensor FET chips to concentrations of aqueous electrical ions and pH of buffer solutions. The present scheme is distinguished from other CNT sensing methods as it uses a gate oxide overlayer on top of the CNTs. The sensor chips were exposed to varying concentrations of sodium chloride (NaCl) and standard buffers of different pH. The resulting data were analyzed using a custom-written program to quantify the response and sensitivity of the biosensors.**

***JIndex Terms*— Biosensors, Electrochemistry, Nernst Potential, Oxide-electrolyte interface, Silver-Silver Chloride Electrode**

I. Introduction

The emerging need for portable and more efficient tools for diagnosis and prognosis of diseases, environmental monitoring and pathogen detection has spurred multi-disciplinary research on the development of biosensors. Electronic detection of nucleic acids, proteins, peptides and antibodies involve immobilizing a probe molecule on the sensor and detecting the capture of the complementary target by changes in the electrical behavior of the transistor. However the FET also responds to other electrochemical effects such as the Nernst potential that depends on the concentration of dissolved ions, and the pH in which the balance of H^+ and OH^- species changes the surface charge on the sensor area. It is thus important to understand these effects and this study aims to experimentally characterize our carbon nanotube biosensors' response to varying concentrations of sodium chloride (NaCl), and buffer electrolytes with varying pH levels.

II. The Sensor System

A. Geometry

The Field Effect Transistor (FET) model present in our biosensors is depicted in figure 1. It is similar to an Ion-selective FET (ISFET), with an electrolyte serving as the top gate of the sensor system. The sensors employ carbon nanotubes (CNTs) -- sheets of rolled up graphene that form a hollow cylindrical pathway [1], as the charge carriers. The high carrier mobility and the strong carbon-carbon bonding offered by CNTs make them ideal semiconducting components for ultra-sensitive biosensors [2]. Our design, shown in the package form contains 64 FETs that are multiplexed on a chip.

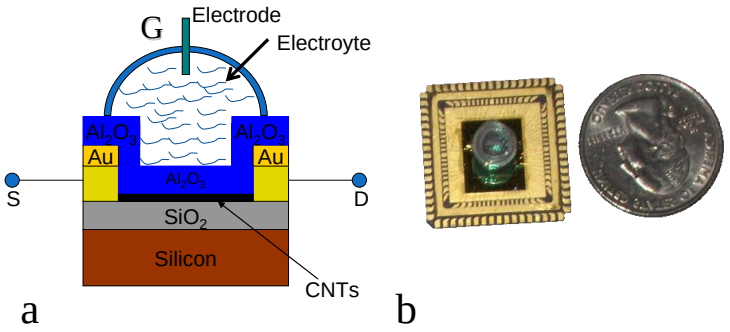

Figure 1: (a) CNT Based FET Model; (b) A Biosensor Chip on Package with Cup for Electrolyte Storage

B. Detection Principles

The theory behind the detection of aqueous ions is well-established in electrochemistry by the Nernst equation, which relates electrode potential to the concentration of the ion surrounding the electrode. It is defined as [3]:

$$E = \mathrm{E}^o - \frac{\mathrm{RT}}{\mathrm{nF}}\ln(\mathrm{Q}) \quad \text{.....(1)}$$

where E is the electrode potential, E^o is the temperature dependent offset potential of the electrode, R is the gas constant, F is Faraday's constant, T is temperature and Q is the reaction quotient of the associated electrochemical reaction.

The measurements on our biosensor chips are made using a silver/silver chloride (Ag/AgCl) electrode. The physical make-up of this electrode includes a silver wire coated with a silver chloride layer. In the context of Ag/AgCl electrode, and assuming operating termperature of 25˚C, the Nernst equation (1) can be generalized to the following:

$$E = \text{constant} - \left(59.16\frac{\text{mV}}{\text{decade}}\right) * \log[Cl^-] \quad \text{.....(2)}$$

where E^o of the electrode is subsumed in the constant term, and $[Cl^-]$ is the concentration of Cl^- ions at the electrode tip.

This equation states that under ideal conditions, every logarithmic increase in concentration of an electrolyte containing Cl^- ions is accompanied by a reduction of the electrode potential by 59.16 mV. We will compare this theory with the results from our sensors by comparing the electrode potential vs. log([NaCl]) plot to the linear relation in equation (2).

The principle behind pH detection follows a different theoretical model. Solutions with varying pH have accordingly varying number of H^+ and OH^- ions. Our biosensors are coated with a layer of Al_2O_3 that shields the carbon nanotubes. The surface of this oxide in contact with the electrolyte contains amphoteric sites that accept the H^+ and OH^- ions from the electrolyte, and become positively charged, negatively charged or stay neutral, depending upon the pH [4]. In addition to the accumulation of the ions on the oxide surface, there is also the concept of double layer capacitance that comes into play in accordance with the theory behind solid-liquid interfaces, in this case the oxide-electrolyte interface [3,4]. This capacitance serves as the load for protonization and deprotonization of the oxide surface. Combining the surface charge development and the double layer capacitance principle, the theoretical model that dictates the principle of pH sensing is given by [4]:

$$\Delta\Psi = -2.3\alpha\frac{RT}{F}\Delta pH_{bulk} \quad \text{.....(4)}$$

Where $\Delta\Psi$ is the change in surface potential introduced by a change in bulk pH (ΔpH_{bulk})of the solution relative to a baseline pH, and α is the sensitivity factor that depends on the value of the double layer capacitance (C_s) and the buffer capacity (β_s) that is intrinsic to the type of oxide. It is given by:

$$\alpha = \frac{1}{\left(\frac{2.3kT}{q^2}\right)\left(\frac{C_s}{\beta_s}\right)+1} \quad \text{.....(5)}$$

where k is Boltzman's constant and q is the magnitude of electronic charge. Assuming operating temperature of 25 ˚C, equation (4) can be now simplified to obtain,

$$\Delta\Psi = -\left(59.16\frac{mV}{pH}\right)\alpha\Delta pH_{bulk} \quad \text{.....(6)}$$

The slope of the change in surface potential with respect to the change in pH of the electrolyte is therefore equal to the Nernst potential described in the Nernst equation seen previously, given that α = 1, which corresponds to large buffer capacity (β_s) and low double layer capacitance (C_s).

Equation (6) predicts the sensitivity to pH, which depends on the type of oxide that is exposed to the electrolyte. This is the guiding equation for pH detection applications of our biosensors.

III. The Experiment Setup

The measurement setup consisting of the peripheral electronics, accessory electrodes and fluid handling is presented in figure 3. The close up photo shows a cut-up PCR tube glued on the chip that serves as the reservoir. The central capillary tube is the silver-silver chloride electrode that carries the gate bias signal, while the other two capillary tubes are fluid pathways for electrolyte delivery and removal.

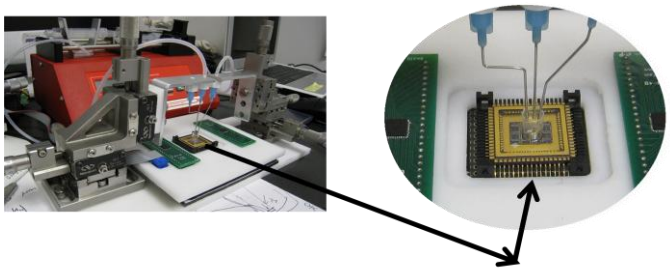

Figure 3: Measurement Setup

For each transistor, the drain-source voltage is maintained at 100 mV, and the gate voltage is ramped while recording the drain current. Custom-written software interfaced with data acquisition electronics records the transconductance curves for further analysis.

IV. Results

Varying concentrations of sodium chloride (NaCl) were applied on one of our chips, W204, while buffer solutions with varying pH were applied on a second chip, W205.

A. *Chip's Response to Varying NaCl Concentrations*

Typical I-V plots and the shift in threshold voltage (Vth) for NaCl concentrations ranging from 5 µM to 5 mM with logarithmic increments are presented in figure 4.

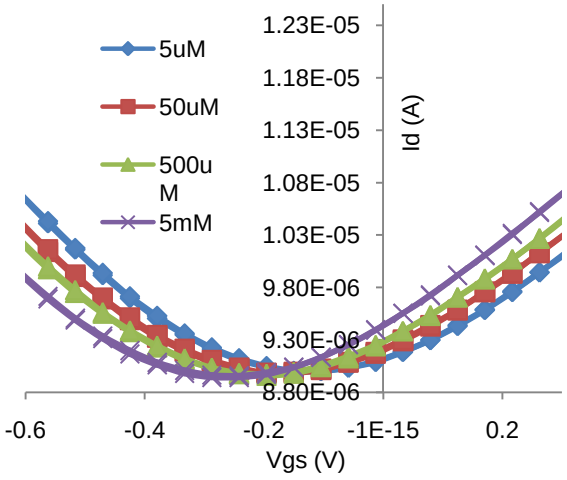

Figure 4: Shifts in Transconductance Curves with Increasing NaCl Concentrations for 1 of 64 FETs Under Test

Five trials of measurements on 64 FETs on the chip were made with each concentration. Threshold voltages (Vth) for all the trials corresponding to each NaCl concentration were

averaged for all the measured FETs. The average of all the resulting trial-specific average, <Vth>, of the FETs was then evaluated. Figure 5 depicts the quantification of the sensitivity to the small NaCl concentrations. The vertical axis shows the relative <Vth>, which is the offset voltage, with respect to <Vth> at 5 µM which we chose as the baseline.

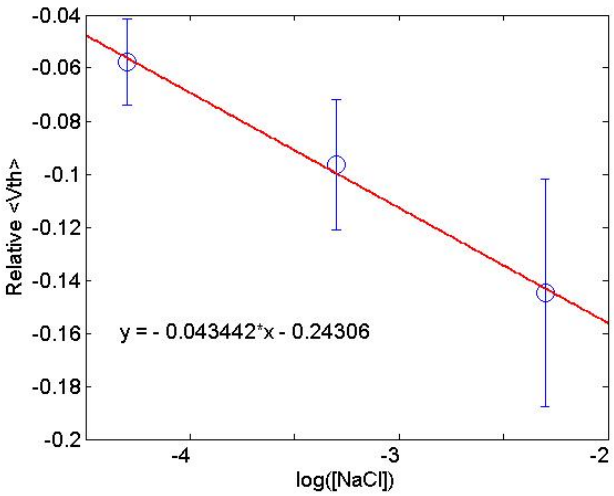

Figure 5: Relative <Vth> from 5µM Baseline

Comparing the linear fit equation from figure 5 to the Nernst equation, the sensitivity to NaCl concentrations for the biosensor is -43.4 mV/decade. This sensitivity calibration compares to the Nernst potential slope of -59.16 mV/decade. Despite the seemingly large difference, this is a very reasonable agreement since the ideal model does not take into consideration possible temperature fluctuations and the Faradic currents, i.e., flow of ions in solution, that could lower the measured potential.

A second set of experiments were performed with NaCl solutions with the objective of improving the error bars of the data in figure 5 by means of improving the voltage sweep precision and evaluating the time dependence of the signal. A single FET from the chip was tested with NaCl solutions of concentrations 50 µM, 5 µM and 500 µM in that order. Figure 6 depicts the trial-dependence relationship of the threshold voltage. In the plot, each trial corresponds to 4 minutes in the time scale. The threshold voltage trend corresponding to 50 µM has been omitted in this analysis since (we discovered later) the system noise was very large after a long pause in the measurement in which the electrode was left dry for a long period of time. The second set of experiments was started after the chip had been idle for about two weeks before 50 µM NaCl was applied on it. Therefore, there is a great likelihood that the sensor took some time to stabilize itself, the result of which was large window of threshold voltage variation.

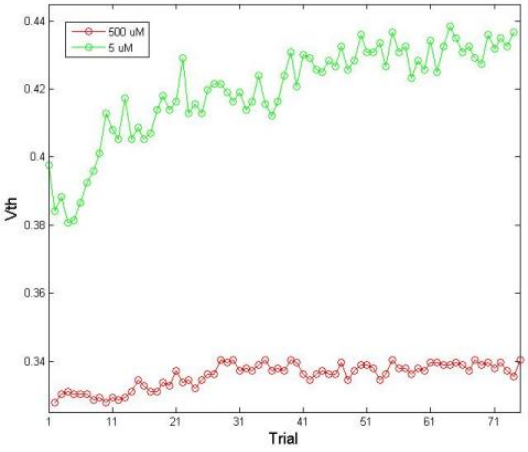

Figure 6: Time Response of an FET to Two Small Concentrations of NaCl

The trend corresponding to 5 µM achieves stability after about eight trials, which corresponds to 32 minutes into the experiment, with voltage variation range limited to 20 mV. The trend corresponding to 500 µM reaches stability after about 27 trials, with very little variation compared to the one seen for 5µM. These observations seem to highlight that larger voltage fluctuations exist at smaller concentrations of NaCl applied on the chip.

The sensitivity calibration result for the second set of experiments is provided in figure 7. Similar to the analysis of the previous experiment set, the baseline concentration was chosen to be 5 µM.

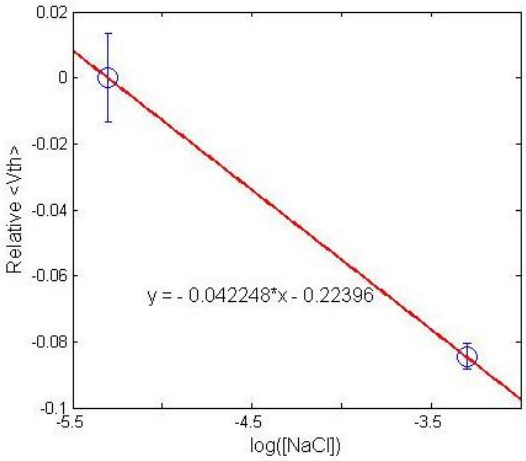

Figure 7: Relative <Vth> from Baseline with Improved Measurement Precision for Two [NaCl] Applied On 1 FET

The resulting sensitivity for the measured FET again, comparing to the Nernst equation, is -42.25 mV/decade. This result is in close agreement with the average sensitivity representative of 64 FETs as seen previously. A 2.69% percent difference exists between the two results.

The plot in figure 7 also depicts a drastic reduction in the error bars associated with the data, as compared to the result from the first set of experiments.

B. Chip's Response to Varying pH of Buffer Solutions

100 trials of I-V measurements were made on one of the FETs on the chip. Typical transconductance curve movement associated with the pH solutions are presented in figure 8. The sensitivity characterization to pH is presented in figure 9.

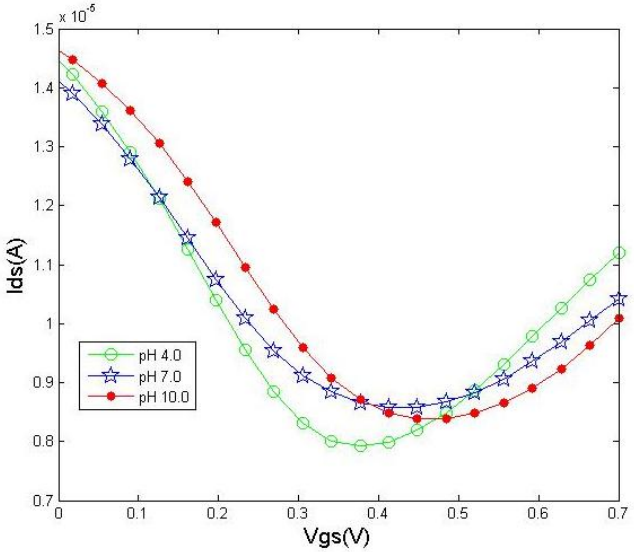

Figure 8: pH Specific Transconductance Curve Shifts for 1 FET

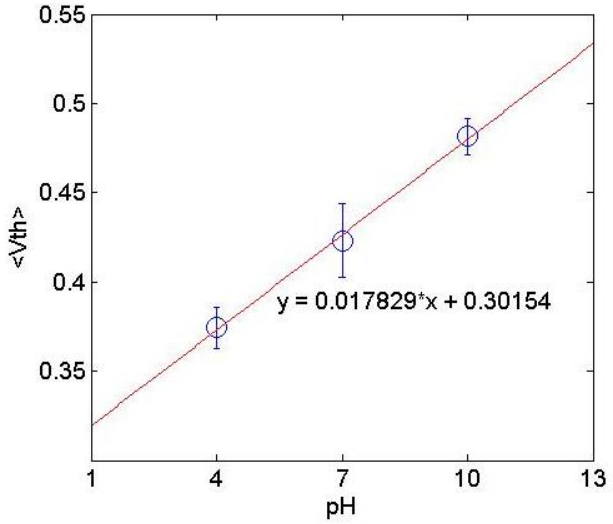

Figure 9: pH Sensitivity Calibration through <Vth> vs. pH of One FET

As seen in this plot, the sensitivity calibration to pH solutions is 17.83 mV/pH.

A second set of experiments were performed with pH solutions with improved measurement precision, so as to evaluate the long-term time-dependence of the threshold voltages. This response for pH 4.0 and pH 10.0 is presented in figure 10.

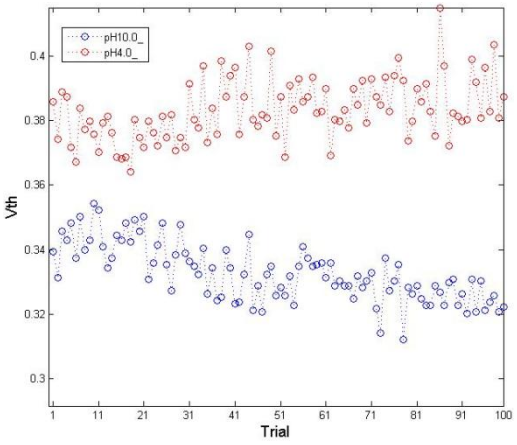

Figure 10: Time Response of One FET to Two pH Values

This time dependence trend seems to contradict with the pH dependence shown in figure 9, from the first set of experiments. There is a great likelihood that this behavior of the trend has to do with the difference in measurement precision. The precision for data collection in the second set of experiments was improved by 80 times, and the pH solution stayed on the chip for six times longer duration of time. While the data for 100 trials on an FET were acquisitioned in 45 minutes in the first set of pH experiments, the second set of experiments took about 5 to 6 hours for completion. As discussed previously, pH sensing relates to changes in charge distribution on the chip surface, which is very prone to distortions and irregularities upon long exposures to high to medium acidity and basicity. This phenomenon is unlike that for NaCl concentrations, where potential fluctuations on the electrode determines detection; hence, time duration for which the solution stays on the chip does not affect the accuracy of measurement as long as the measurements are being made for length of time shorter than the settling time of NaCl salt.

V. Conclusions

Sensitivity of our biosensor to small concentrations of NaCl solutions ranging from 5 µM to 5 mM were experimentally characterized to be -43.4 mV/decade. In second set of experiments, the sensitivity of one FET on the chip was found to be -42.25 mV/decade, within 2.69% error compared to the sensitivity for the overall sensor. Time-dependence of a representative FET on the sensor was experimentally determined. Larger voltage fluctuations with time were observed at smaller concentrations of NaCl.

Sensitivity of an FET in a second biosensor chip to buffer solutions with three different pH values was found to be 17.83 mV/pH.

VI. Future Work

We will carry out additional experiments with a larger sample of pH on both acidic and basic sides, with the most optimal and practical measurement precision in order to establish, more definitively, the sensitivity to pH. This set of experiments will be performed on all the 64 measurable FETs on the chip in order to get a bigger picture of the biosensor's

operation. A rigorous error analysis of the currently obtained results for both NaCl and pH, with inclusion of the device parameters will also be performed.

VII. Acknowledgements

Sincere thanks to the NSF Award # 0755224. Heartfelt thanks to Konrad H. Aschenbach, Dr. Romel D. Gomez, Dr. Pamela Abshire, Laboratory of Physical Sciences (LPS), the Maryland Nanocenter, and the MERIT/TREND/CS peers.

References

[1] N. Sinha, J. Ma, J. T. W. Yeow, "Carbon Nanotube-Based Sensors," in *Nanoscience and Nanotechnology*, vol. 6. 2006. pp. 573-590.

[2] K. H. Aschenbach, H. Pandana, J. Lee, J. Khan, M. Fuhrer, D. Lenski, R. D. Gomez, "Detection of Nucleic Acid Hybridization via Oxide-Gated Carbon Nanotube Field-Effect Transistors," *Proceedings of SPIE* 18-20 March 2008. vol. 6959.

[3] Wikipedia, the Free Encyclopedia, "Nernst Equation," http://en.wikipedia.org/wiki/Nernst_equation. Date Retreived: 07-20-2009

[4] P. Bergveld, "Thirty Years of ISFETOLOGY: What Happened in the Past 30 Years and What May Happen in the Next 30 Years," in *Sensors and Actuators*, 2003. pp. 1-20.